EIGHT EUROPEAN ROTORCRAFT FORUM

Paper No 12.6

LOW LEVEL FLIGHT AND NAVIGATION AT NIGHT IN CENTRAL EUROPE

W. METZDORFF, H. HAUCK

DORNIER GMBH

August 31 through September 3, 1982

AIX-EN-PROVENCE

ASSOCIATION AERONAUTIQUE ET ASTRONAUTIQUE DE FRANCE

1. HUMAN PILOT VISION INFORMATION PROCESS

The NOE-flight ($H < 100$ ft, $v = 0 \ldots v_{max}$) is close-contact-to-topography flight. The pilot gains all flight information necessary for guidance and control of the aircraft optically. The landscape consists of topographic objects (houses, streets, wood, rivers, ...). The objects are mainly recognisable from geometric features as shape, size, surface texture etc. The reflected energy from the illuminated topographic objects/features generates a twodimensional contrast image on the eye's retina. The human brain extracts the features and compares against the human internal object/feature reference memory, thus performing the recognition of scene objects (see figure 1). The understanding and interpretation of the scene and the associated scene changes lead in the subsequent human process to the estimation of all flight states necessary for guidance and control of the NOE-flight. The most important references (objects/features), recognisable by a pilot, and the respective estimated flight state informations are listed below

- o Horizontal and/or vertical reference lines (houses, trees, ...)
  attitude in roll, attitude in pitch
- o Perspective and rate of change of perspective of surface structures
  altitude, ground speed, attitude
- o Perspective, size (scale) and shape of objects
  range, separation, obstacle clearance

For close contact vision, an at least sufficient object/feature contrast, is the key element for the pilot's capability, performing close contact flight. The flight state information from the topographic scene is augmented by the flight state information derived from sensors and displayed in symbolic features (symbology) in the cockpit scene. With decreasing contrast in the topographic scene, the decreasing flight state information is augmented/substituted by the flight state symbology to a certain extent. Below a certain contrast threshold no further NOE-flight is possible. The flight state information through the displayed cockpit symbology then only provides normal instrumental flight conditions which are not as close to the terrain as required for NOE-flight.

2. SURVEY OF NIGHT VISION TECHNOLOGIES

For close contact night flight, the visual topographic scene information with sufficent contrast for flight state estimation has to be provided through a NIGHT VISION SYSTEM NVS.

At night, the scene image generally is made visible in a display through radiation amplification and/or wavelength conversion by the NV sensor. Present and future technical solutions are listed in table 1 showing detection wavelength and operating mode of the respective device. Of present practical importance are image intensifier systems (LLLTV, NV-Goggles) within the visible range (0.4 ... 0.7 µm) and image converter systems (FLIR) within the infrared range (3 ... 5 µm and 8 ... 12 µm). Systems are referred to as being passive, if no artificial illumination of the scene is performed. The additional future solutions listed in the table will be discussed briefly in the outlook chapter.

The vision information provided by a NVS is limited by different effects. They might be roughly divided into:

- o systematic geometric effects/parameters as
  geometric resolution, field of view, direction of view, image scale, line of sight stabilization
- o statistical geophysical effects/parameters as
  material absorption, reflection, emission
  atmospheric physical effects depending from weather conditions

The geometric parameters are inherent in the specific equipment solutions and will be briefly mentioned in the later comparison. Consideration has to be given here to the geophysical effects, causing a statistical time variance of the sensed and displayed contrast of the objects/features in the NV image. Of most interest for the purpose of performance comparison is the probability of occurence of those effects which decrease the sensed object contrast in the displayed scene to the threshold where no further recognition and flight state estimations take place.

There is no simple conclusive answer available up to now. The use of mean year values for the probability of occurence of specific weather effects is not advisable because of the season/night time and regional differences. Here, in a very simplified manner, at least major effects will be discussed with the aim of providing some contrast in understanding.

3. CONTRAST AND CONTRAST LIMITING EFFECTS

The intrinsic contrast $C_i = (e_1 - e_2)/e_1$ is the contrast between different surfaces where e_1, e_2 is given in terms of energy density $e\,[Wsm^{-2}]$ and expressing radiant flux in the respective wavelength region.

For $\lambda < 3\ \mu m$ the principal component of radiation observed in the visible (0,4 ... 0,7 μm) and near infrared (0,7 ... 3 μm) is reflected energy. It depends upon the level of irradiation/illumination and on the reflectivity of the objects, fig. 2, ref. 1.

$$e(\lambda < 3\ \mu m) = f[\text{illumination, reflectivity}]$$

For $\lambda = 3 \ldots 15\ \mu m$ the principal component of observed radiation in the middle and far infrared region is emitted energy. It depends upon temperature and emissivity of objects, fig. 3.

$$e(\lambda = 3 \ldots 15\ \mu m) = f[\text{temperature, emissivity}]$$

If in the first order the reflectivity* and the emissivity properties of the materials are considered constant then variations in the observed radiated energy and the subsequent variations of the intrinsic contrast C_i are caused mainly by

---

*Reflectivity and emissivity of the natural topographical objects show seasonal dependance. As an example the seasonal changes in the spectral reflectance of oak leaves are shown in fig. 4.

variations in irradiation/illumination levels ($\lambda < 3$ µm) and the temperature differences ($\lambda = 3 \ldots 15$ µm)

C_i ($\lambda < 3$ µm) illumination threshold
C_i ($\lambda = 3 \ldots 15$ µm) temperature difference

For $\lambda < 3$ µm (energy reflection) the aparent contrast C_a at the observation site is different from the intrinsic contrast C_i of objects at a distance due to two major propagation effects shown in fig. 2.

- o Some of the energy emanating from distant objects is selectively removed from the line of sight transmission path by absorption and scattering (transmission attenuation).
- o Some energy is selectively added as path radiance, mainly produced by scattering in the line of sight (adding noise).

For $\lambda = 3 \ldots 15$ µm (emission) the propagation effects, fig. 3, are the same but with the exception, that the path radiance here is mainly produced by atmospheric emission (adding noise).

If the transmittance in a simplified model is considered as the main atmospheric propagation parameter, the following effects, which might result in image degradation down to no NV visibility have to be covered for completeness.

- o $\lambda < 3$ µm (LLLTV/NV-GOGGLES)
  - Ambient scene illumination
  - Atmospheric transmission
- o $\lambda = 3 \ldots 15$ µm (FLIR)
  - Low scene temperature differences (thermal contrast)
  - Atmospheric transmission

Environmental effects are not at all independent of each other but are strongly coupled.

4. ATMOSPHERIC TRANSMISSION

For reasons of comparison between the NVS for the visible region (LLLTV and NV-GOGGLES) and for the infrared region (FLIR) the contrast transmission $\tau = C_a/C_i$ [%] for a transmission path from the scene objects to the observation site will be considered.

The transmission through the atmosphere, fig. 5, for wavelength from 0,2 ... 15 µm has been calculated for a 1 km horizontal path with the LOWTRAN5 model, ref. 2, for different visibilities v_N as parameters. The transmission as a measure of atmospheric transparency mainly depends on the size and amount of the various constituent particles in the air. For a visibility of $v_N = 50$ km the atmospheric transparency is in all windows high and the transmittance decreases over the whole spectrum by only about 10%. Values in Fig. 5 are for the visible region 0,4 ... 0,7 µm $\rightarrow \tau \sim 90\%$ and in the infrared region 3 ... 5 µm $\rightarrow \tau \sim 90\%$, 8 ... 12 µm $\rightarrow \tau \sim 80\%$. For the more likely realistic visibilities $v_N = 5$ km down to $v_N = 0.3$ km the situation changes. For $v_N = 5$ km the transmittance in the infrared region is still high (75 ... 85%) but has been decreased in the visible region down to 55%. For additional decrease in the visibility (i.e.: increase in humidity), the transmission will for the shorter wavelength < 3 µm decrease much faster compared to the longer wavelength i.e.: at 4 µm or 10 µm.

The transparency of the atmosphere within the infrared region is therefore much better compared to the visible region. In fig. 6 the average transmission for the respective wavelength regions have been plotted against visibility v_N. For 1 km visibility the transmission in the infrared region is better by a factor of 14 ... 27 and for 2 km still by a factor of 3 to 5.

Since the transmission of the atmosphere for NVS is more restricted in the visible region (LLLTV/NV-GOGGLES) in comparison to the infrared region (FLIR), the frequency of occurrence of these restrictions in Central Europe are of interest. Date of seasonal variations for the visible and infrared transmittance and their frequency of occurrence for Central Europe might be drawn from the NATO OPAQUE PROGRAM, ref. 3 (classified). Here the frequency (probability) of occurrence for certain visibility measures, ref. 4 are used instead.

The statistics shows that with an average frequency of about 90% the visiblity in Germany is $v > 1{,}8$ km, that no restrictions of the NV visibility paths can occur due to the atmospheric transmission. For the remaining 10% lower visibility cases occur and the different NV solutions will be differently limited by atmospheric transmission. More detailed information might be taken from fig. 7, where the frequency of occurrence of the lower visibility cases $v < 1{,}8$ km is split in cases (from top to bottom) for $v < 0{,}5$/$v = 0{,}5$ ... $0{,}9$/$v = 0{,}9$ ... 1,8 km. A rough estimation leads to the following categories

VISIBILITY	AVERAGE OCCURRENCE	LLLTV/NV-GOGGLES	FLIR
For v < 0,5 km,	3%	no NV	no NV
For v = 0,5 ... 0,9 km	1,7%	no NV	poor NV
For v = 0,9 ... 1,8 km	4,5%	poor NV	NV

The seasonal variations from the given average might be deduced from the respective diagrams. The frequency of poor NV or no NV is considerably greater in the fall and winter than in spring and summer.

5. ILLUMINATION

For wavelength $\lambda < 3$ µm the intrinsic scene contrast is down sufficiently to the threshold of ambient irradiance. For LLLTV and NV-GOGGLES the ambient irradiance is the illuminance for the visible region (0,4 ... 0,7 µm) with little extention to the near infrared up to 1 µm.

In fig. 8 the level of the scene illumination at the night hours* is drawn for the two extrem conditions, i.e. for a short summer night with full moon and a long winter night

*Night hours - are defined as the time from half an hour after sunset until half an hour prior to sunrise without moon , ref. 5. The magnitudes of illumination at night times occur within these limits. Both cases are indicated with "sky clear" and "overcast" weather conditions. Statistical estimation shows, that along German geographic latitudes the night times make up approximately 45% of the local time. About one third of the night times; i.e. about 15% of the night times, the minimal sky illuminance situation occurs. At this frequency of occurrence which depends on the cloud cover, the level of illumination is about 0,5 mlx. This is the illumination threshold required for sufficient contrast for the NV-GOGGLES of the third generation. Thus, it can be concluded, that no significant limitations due to the scene illuminance exists.

The performance of the NV-GOGGLES of the third generation have been significantly improved compared to the performance of the second generation. The upper diagram in fig. 9, ref. 6, shows the improvement in the sensitivity (logarithmic scale). Here, most important is the extension to the near infrared because the average ambient radiance is of greater magnitude in that region (middle diagram). In addition the average reflectivity of topographic objects (bottom diagram) also increases.

6. THERMAL CONTRAST

At wavelength beyond 3 µm the radiation from the topographic objects/features is dominated by self-emission, which depends on the temperature of the objects/features and or their emissivities. Table 2 lists emissivities of some typical topographic objects/features in the infrared region, ref. 7. This table clearly shows that most objects beyond 3 µm will have an emissivity greater than 0.8.

In the daytime the temperature of the terrain objects is related to their optical properties in the visible and infrared regions, to their thermal contact with the air and their heat conductivity and heat capacity.

The cooling rate of the terrain objects at night time will depend on the following
o heat capacity
o heat conductivity
o thermal contact with the surrounding air
o infrared emissivity
o atmospheric humidity
o cloud cover
In a very dry location when their is no cloud cover, all the thermal radiation in the 8 .. 12 µm region will be radiated into space and the objects will cool down rapidly, table 3. Vegetation which is in close contact to the surrounding air, and water surfaces which have large heat capacities will radiate during the day and the night.

Of particular importance will be to know the times during the day and at night when the spectral radiance from different terrain objects/features are identical to give minimum contrast. These times are referred to as crossover-times. Measurements of crossover-times of terrain-objects/features have been made and these times are found to vary widely depending on the objects considered. As an example fig. 10, ref.7 shows the relative contrast of deciduous trees to short grass. The crossover-times are shown in hours relative to sunset and sunrise and for the four seasons.

Other reasons causing minimum contrast are severe cloud coverage for longer times, rainfall and high degree of air humidity (thick fog). There is presently no chance to include all the effects mentioned in a simple enough model to give conclusive answers for the degree of degradation of the contrast in correlation with the frequency of occurrence of all these effects.

In the following, some experimental results on specific thermal contrast situations will be discussed. Fig. 11 presents an image from a thermal contrast situation which was considered by the pilots as being good. Fig. 12 shows a similar scene with the same objects (houses) at a poor thermal contrast situation which was considered by the pilots as the lowest NV limit. The analysis of the poor image in the image processing laboratory resulted in a signal to noise ratio of about 3. The number of discernable shades of gray with minimal resolvable contrast was counted as 8, see histogram fig. 14. The corresponding intensity resolution therefore is described by 3 bit. This gives an indication of the lowest required aparent contrast conditions. As a comparison, the image from good contrast conditions, fig. 11, has a signal to noise ratio of about 80 and about 40 discernable shades of gray (5 to 6 bit intensity resolution). (The measured noise was frozen noise from the static image. For the human observer of a 25 frames per second picture the dynamic noise is less effecting).

To the poor contrast image of fig. 12 a contrast enhancement has been applied. The effect of the operation is to "stretch" the gray scale from the relatively narrow, middle-range picture on the original to a full contrast image with gray values ranging all the way from 0 ... 255, i.e. 8 bit intensity resolution. The resulting image is shown in fig. 13.

Other image enhancement methods are mentioned in the last chapter with reference to the images from fig. 23 to fig. 27.

7. PRACTICAL EXPERIENCE WITH NIGHT VISION SYSTEMS

Within the last five years, Dornier has gained practical experience with different NVS solutions.

- o FLIR-HMD-HMS
- o FLIR-PMD-automatic and/or manual LOS-control
- o NV-GOGGLES

Since December 1981 Dornier runs another flight test program together with the German Forces Flight Test Center to examine an Integrated Helicopter Nightflying System consisting of

- o Mini FLIR/Platform (NV-GOGGLES as safety system), PMD
- o Display augmentation system
- o Doppler augmentation system
- o Doppler navigation systen and a
- o Flight management system.

The experimental system is installed in a Bell-UH-1D helicopter. The blockdiagram of the system installation is shown in fig. 15. The test bed helicopter with the stabilized FLIR are shown in fig. 16/17 and the test pilots station in fig. 18. The installations at rear fig. 19 are operated by the flight test engineer and the navigator.

The principal objectives of the flight experiments are

- o To assess the real sensor performance taking into account season, daytime, terrain and weather effects in Central Europe
- o to verify or correct the previously designed display augmenting symbology
- o to check the feasibility of navigation together with a Night Vision System i.e.
  - waypoint identification
  - update procedure etc.

For the flight tests five very experiencedpilots directly involved in the program (2 Testpilots, 3 Airforce IP's) have been at our disposal. To give some impression of the flight experiments a videotape has been prepared supporting the oral presentation. The following features mentioned will be shown in the video presentation.

- o Experimental System hardware
- o Manoeuvres, Missionphases
  - take off
  - departure
  - cruise
  - navigation aspects
  - hover
  - touch down

Although the flight test program will continue till November 1982 and the final results are not yet available, some practical experience with the Night Vision System Configurations shown in fig. 20 are being discussed. The discussion is being performed refering to the mission outlined in table 4.

8. FLIR, HMD, HMS

With the HMD's the pilot is not restricted in his selection of direction of view. The co-pilot with the FLIR image displayed on an additional PMD has to get along with a picture directed by the pilot, which is a disadvantage. The scale factor for FLIR viewing angle with respect to the eye's viewing angle is approximately unity. This has been proven as an ideal situation because no errors in estimating range, separation and direction do occur. All three mission profiles have been proven to be feasible.

9. FLIR, PMD, LOS-CONTROL AUTOMATIC/MANUAL

The automatic/manual control of the direction of view gives some restrictions if the complete angular range of DOV by manual control is utilized a side view or top view on a front view display will be found. But this effect does not confuse pilots in normal operation because the usual direction of view is close to a reference angle of 0° Azimut and -10° Elevation. The most frequent angular range is around ± 15° Azimut and ± 10° Elevation relative to this reference angle. The relevance of the restriction appears with decreasing height because the judgement of clearance of flight path gets increasingly difficult especially in terrain avoiding manoeuvres.

The scale factor for FLIR/eye viewing angle is approximately 0.5 (broad angle of view relation). Estimation errors do occur.

- Estimation of range/separation is slightly in the safety critical direction
- Estimation of side range is in the safe direction

The configuration allows mission I without any restrictions to be performed. Mission II flight is possible with extensive mission planning preparation. Mission III can be performed only with extensive mission planning preparation for a wellknown route.

10. NV-GOGGLES, PMD (SYMBOLOGY)

From the operational point of view, the NV-GOGGLES solution is most suitable because the pilot and the copilot gain independently their night vision images for both eyes. All the procedures are most similar to daylight (VMC) operations. Each direction of view can be independently realized. By the incorporation of the NV-GOGGLES to the pilot's helmet (conducted by the German Army Aviation School) the distance from the optics to the eye has been increased. The eye retina's image is scaled down. The image scale factor is approximately 0.8, which leads to small but still evident errors in range estimations. The spatial resolution and the viewing angle (48° circular) are appropriate for all missions. As the most important disadvantage might be considered that frequently occurrence of peak lights in the scene together with low illumination levels leads to eye adaption difficulties. In case of conflict night vision countermeasures have been taken into consideration. The use of the NV-GOGGLES is operationally not possible for visibility ranges less than 1.5 km. In case of appropriate visibility range and scene illumination, above the threshold all of the three defined mission profiles can be successfully performed.

11. NAVIGATION FOR LOW LEVEL NIGHT FLIGHT

For low level night flight an autonomous basic navigation system with an accuracy of distance traveled of better than 0,7% together with a navigation map display is essential. Considering the basic system accuracy, a terrestrial update has to be performed every five to ten minutes. This update is easily performed by the pilot taking the scene information from the NV image. However a thorough mission planning is required to select waypoints with sufficient features which can be easily identified. This is always the case when a combination of objects/features occurs within a favorable spacious arrangement.

Though important obstacles are often recognized in time with the NVS, the problem of obstacle detection has not been completely solved yet. For small objects the spatial and the contrast resolution of the NVS is insufficient since the position of major obstacles are known during mission planning, the flight path can be arranged to save obstacle clearances. The NVS allows verification of obstacles having passed even when the early detection is impossible.

12. DISPLAY AUGMENTATION SYMBOLOGY

As already discussed, the contrast of NV images is not stationary and can be degraded severely. Thus the terrain objects/features are not accessable to the pilot and flight states estimates are therefore insufficient. Depending on the scene information content even with a reasonable good NV image no contrast information might be available. For the low altitude flight over an uniform terrain (extended field, forest) and within a limited field of view, no objects/features can be displayed for flight state estimation. At this point the information for the pilot has to be augmented by the flight states information, derived from sensors and displayed in symbolic features (symbology) to compensate for NV image deficiencies.

Although symbology of all the flight states is displayed, the pilot still has to estimate ranges, separations and obstacle clearances from the NV image. Likewise the navigation update data are only determinable from the NV image. Under moderate to poor contrast and scene feature conditions the symbology has to support the NV image information. In the cases of severe degradation of the image it has to allow the guidance and control of the helicopter as under instrument flight conditions.

In the Dornier experimental program, the already existing cruise symbology, fig. 21 is further improved with the objective to develop a symbology layout which can be applied universally and to cover all flight profiles from hover, fig, 22, to instrument flight, with only little changes to the layout. The video film in the oral presentation will provide an impression of the display augmentation symbology.

13. FUTURE NV TECHNOLOGY IMPROVEMENTS

For light amplification devices (LLLTV/NV-GOGGLES) no more significant improvements can be foreseen, as far as the electro-optical devices are concerned. Solutions of blending the flight states symbology into the viewing channel of the NV-GOGGLES are being furter pursued. Other solutions for presentation of the symbology are on the Head Up Display HUD or on the Panel Mounted Display PMD. For direct viewing of the symbology through the GOGGLES the symbology should be focussed at infinity.

Other activities are to improve the FLIR electrooptics. Here most important is the development of self-scanned detector arrays or matrices with increased thermal resolution. FLIR systems without the mechanical scanning complexity are then possible. All improvements are aiming to improve the range of applications where todays devices are still restricted. Furthermore, the new technology of IR Charge Coupled Devices (IR CCD) are promissing to decrease cost, weight and volume.

Further and essential improvements can be achieved with digital image processing methods to enhance images in real time. The series of images from fig. 23 to fig. 27 demonstrates the effects of different processing cycles and filtering methods, being applied to an optical image (The picture shows a part of the DORNIER facilities at Lake of Constance).

The first series of four images in fig. 23 shows the effects of spatial and intensity qualization, the first step in digital image processing. The original image contains 98000 pixels, each pixel representing one of 64 intensity levels/shades of gray (i.e. 6 bit from black to white). The effect of the reduction of the number of intensity levels is demonstrated in the upper right image, the number of intensity levels is reduced to 8 (3 bit). The reduction of spatial resolution is shown in the bottom left image, here the number of pixels is decreased to 6000. Both, the reduction of spatial resolution and intensity levels is shown in the last image (bottom right). In a careful analysis the appropriate quantization for the subsequent enhancement process has to be determined. This analysis is needed only to process valid sensor information, to reduce computer complexity and to improve image enhancement speed for real time applications. The following images in fig. 24 to 27 show different enhancement operation. Each set of two images is a comparison, the lower image showing the effect of enhancement applied to the upper image.

All the considered improvements will be limited by inherent passive Night Vision Systems performance. These is the thermal noise in the detecting semiconductor materials, limiting the intensity/thermal resolution. Furthermore, system performance is also limited by scene illumination and thermal contrast, as well as the atmospheric attenuation. An alternative NV technology might be found in lower wavelength regions of the electromagnetic spectrum, down in the mm Waves (1 ... 4 mm), table 1. Another approach could be the step to active imaging systems. Here, as an example, an image gained from a feasibility experiment is shown in fig. 28. The bottom image is the normal visual image of the scene shown for comparison. The upper image is a so called range image from a scanning puls laser radar (LADAR). The scanning LADAR measures the range/distance to each scene element within the spatial resolution of the system. The range values are coded in shades of gray for human perception. This image contains all geometric relations for a well trained interpretor. The development of such technologies might overcome several short-comings of the passive NV solutions. In addition the still existing problems of obstacle detection for close contact flights might be solved.

REFERENCES

1. Dieter H. Höhn, Introduction To Optical Problems of Systems, AGARD Lecture Series No 93, Advances In Radio And Optical Propagation

   J. Albertz, W. Kreiling, Photogrammetric Guide, Herbert Wichmann Verlag Karlsruhe

   E.K. Seyb, A Mathematical Model For The Calculation Of Visual Detection Range, Technical Memorandum TM-152, SHARE TECHNICAL CENTRE

2. Atmospheric Transmittance/Radiance, Computer Code LOWTRAN, Optical Physics Division, AFGL Airfoce Geophysics Laboratory, Hanscom AFB, Nassachusetts

3. R.W. Fenn, E.P. Shettle, Atmosperhic Optical/IR Properties In Northern Germany, AGARD Conference Proceedings No. 300, Special Topics In Optical Propagation

4. A.H. Green, L. Parrish, R.G. Haraway, Cloud and Weather Data For Preliminary Evaluation Of Proposed Sensor Guidance Applications, Special Report RE-82-2, Advanced Sensors Directorate, US Army Missile Command, Redstone Arsenal, Alabama

5. Kalender der nächtlichen Globalbeleuchtungsstärke zur Nachthelligkeitsvorhersage 1. und 2. Quartal 1982, Amt für Wehrgeophysik, BU Geophys. BDBw No. 19

6. Edward J. Sheehan, Survey of Present Combat FLIR Designs And Equipment, Electro-Optical Systems and Technology, Conference Documentation 1981

7. Khalil Seyrafi, Editor, Engineering Design Handbook On Infrared Military Systems, AMCP 706-127, Headquaters, US Army Material Command

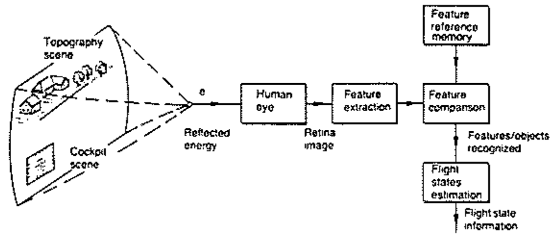

Fig. 1 Vision Information Process

Electro-magnetic wavelength	Passive Energy image	Active Energy image	Active Range image
0,35...0,75...1 µm	LLL-TV NV-Goggles	→	Ladar-R
3...5/8...12 µm	FLIR	→	Ladar-R
1...4 mm	Radiometer	Radar-E	Radar-R

Table 1 Night Vision Techniques Overview

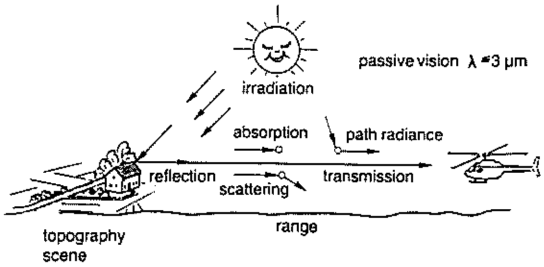

Fig. 2 Atmospheric Optronical Propagation Effects

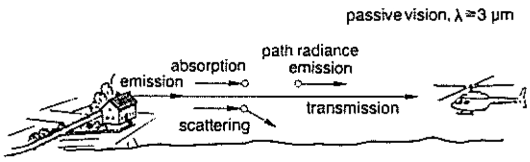

Fig. 3 Atmospheric Optronical Propagation Effects

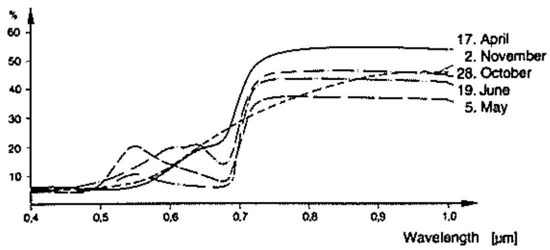

Fig. 4 Seasonal Spectral Reflectance Oak Leaves

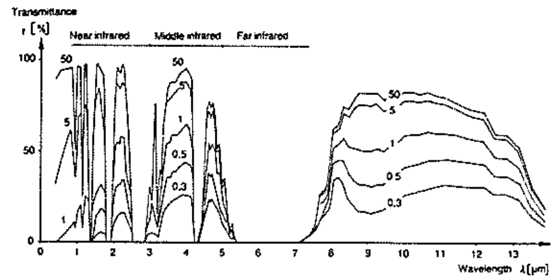

Fig. 5 Atmospheric Transmittance Versus Wavelength, Lowtran 5, Midlatitude Summer, 1 km Path, 500 m GND Parameter: Visibility V_N (km)

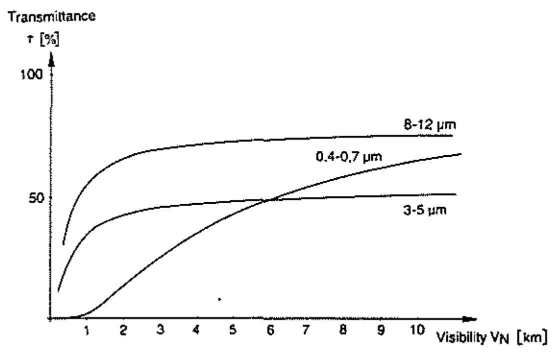

Fig. 6 **Average Transmittance Versus Visibility, 1km Horizontal Path, 500 m GND, Lowtran 5, Midlatitude Summer**

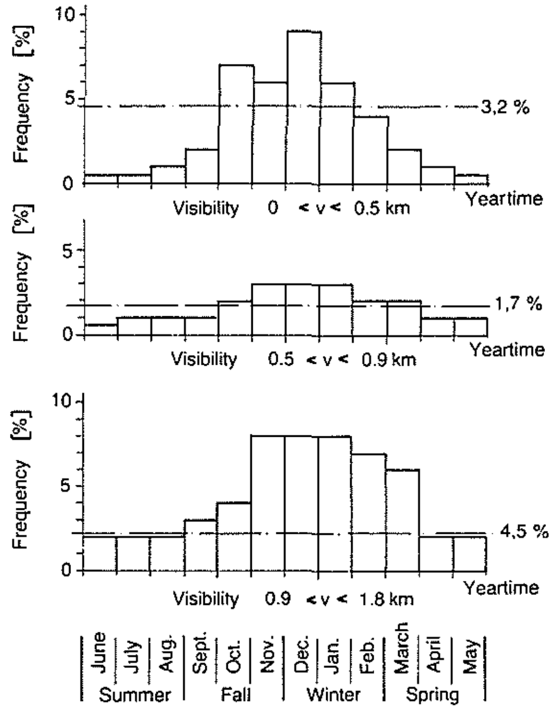

Fig. 7 **Frequency of Occurance of Low Visibilities**

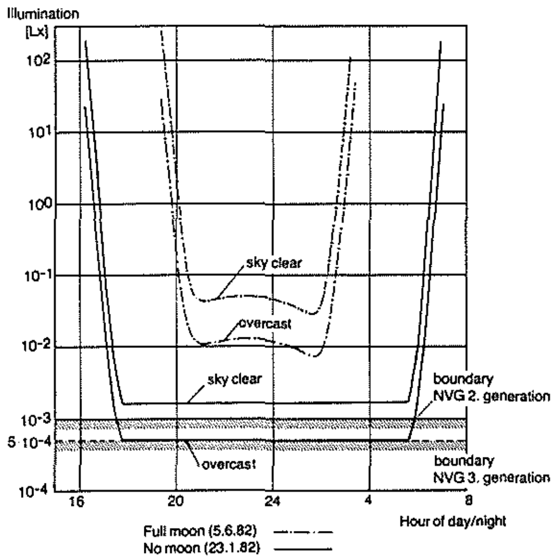

Fig. 8 **Scene Illumination at Night (49°N, 9°E)**

	1,8–2,7 µm	3–5 µm	8–14 µm
Leaves	0,58–0,86	0,86–0,96	0,90–0,97
Sand	0,54–0,82	0,74–0,90	0,92–0,98
Bark	0,69–0,78	0,87–0,90	0,93–0,97
Grass	0,62	0,82	0,88

Table 2 **Emissivity ϵ of Common Terrain Features**

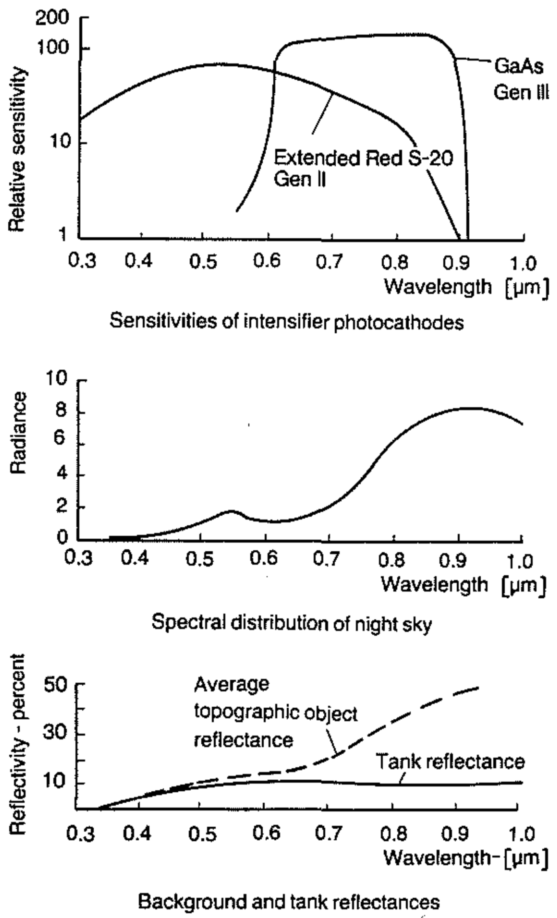

Fig. 9 **Performance Criteria of Night Vision Goggles Third Generation**

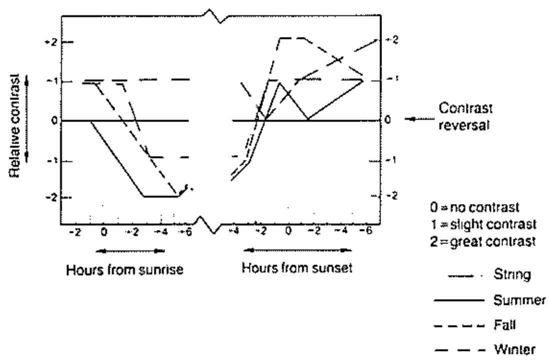

Fig. 10 Relative Contrast of Deciduous Trees to Short Grass ($\lambda > 4\ \mu m$)

Date 24. 3. 82, Sunset 17.35 Z					
Observation time GMT	16.50	18.15	18.50	19.50	20.50
Windspeed kts	calm				
Visibility km	8.5	7.4	6.7	6.2	5.0
Air temperature C	8.2	2.5	0.4	-0.2	-1.2
Weather	Sky clear				
Radiation temperature C					
House wall, east side	12.5	10.2	9.7	9.0	8.2
House wall, west side	21.0	14.5	13.2	12.4	11.4
Concrete roof	20.2	16.0	14.5	13.8	12.7
Metal structure	19.2	9.5	8.2	7.0	6.0
Ploughed field	11.5	7.5	6.0	6.5	7.0
Meadows	9.5	5.0	4.8	5.0	4.5
Forest edge	14.5	10.0	9.5	9.2	8.7
Road (asphalt)	12.6	10.2	10.0	9.2	8.5

Table 3 Radiation Temperature

Fig. 11 FLIR Image Good Contrast

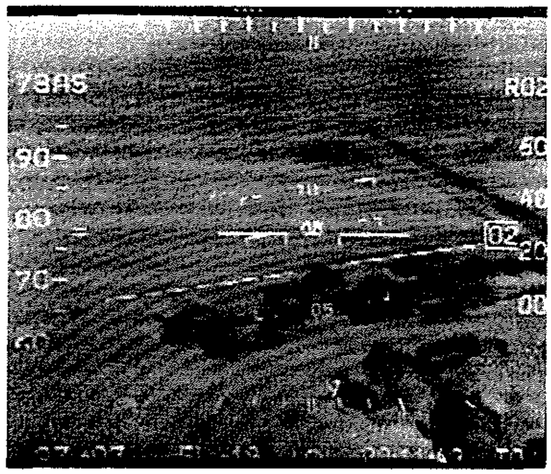

Fig. 12 FLIR Image Poor Contrast

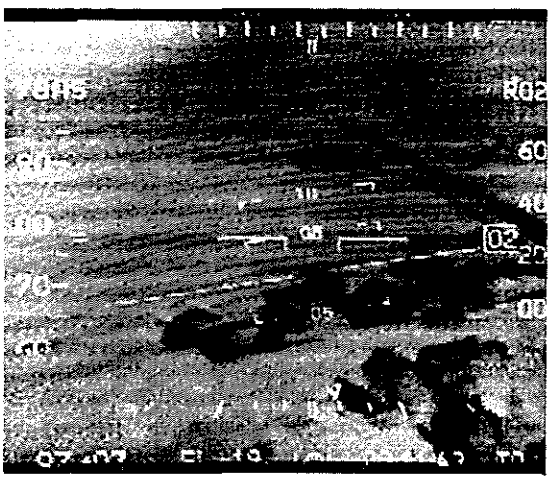

Fig: 13 Contrast Enhancement

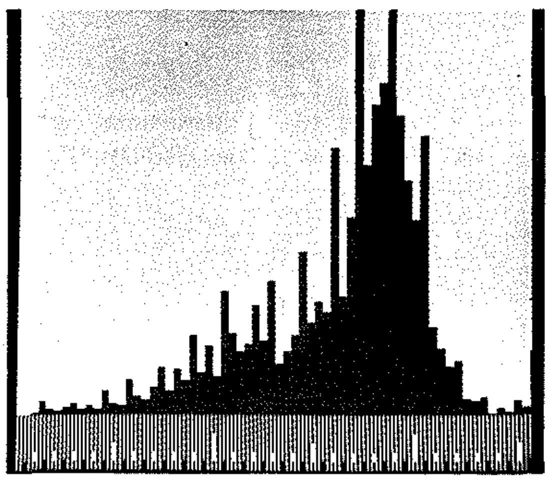

Fig. 14 Histogram

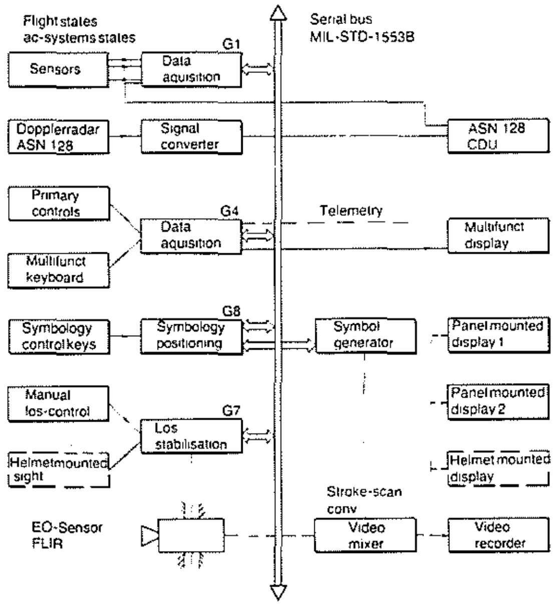

Fig. 15 NSC Experimental System Blockdiagram

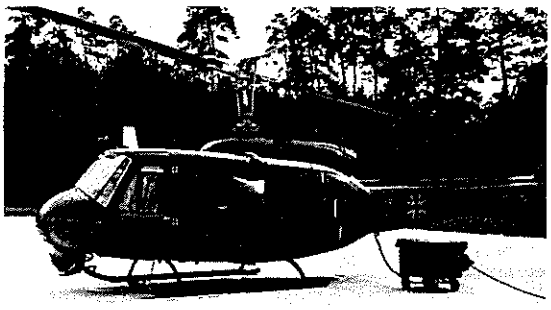

Fig. 16 Experimental Test Bed UH-1D

Fig. 17 Gimballed FLIR-Platform Installation

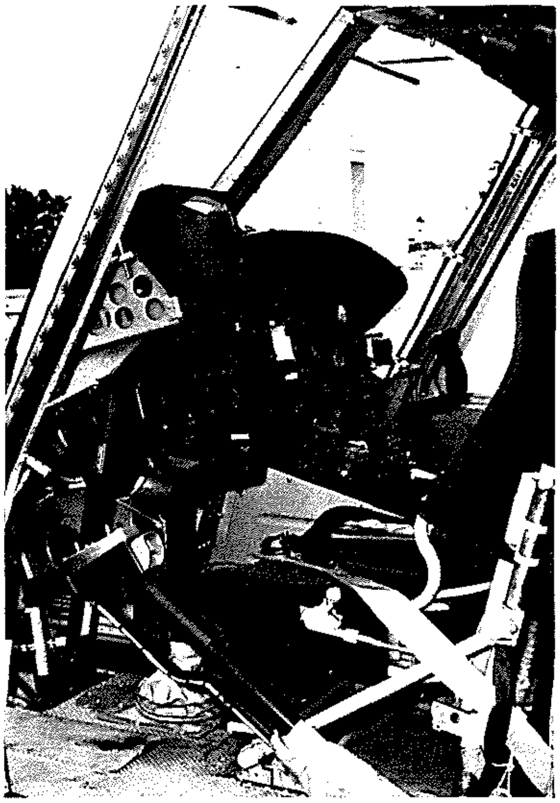

Fig. 18 Experimental Test Pilot Station

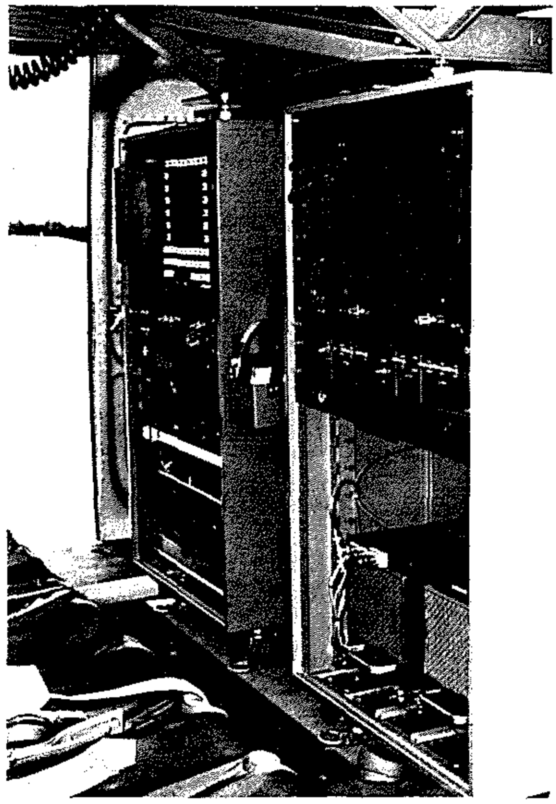

Fig. 19 Test Engineer and Copilot/Navigator Station

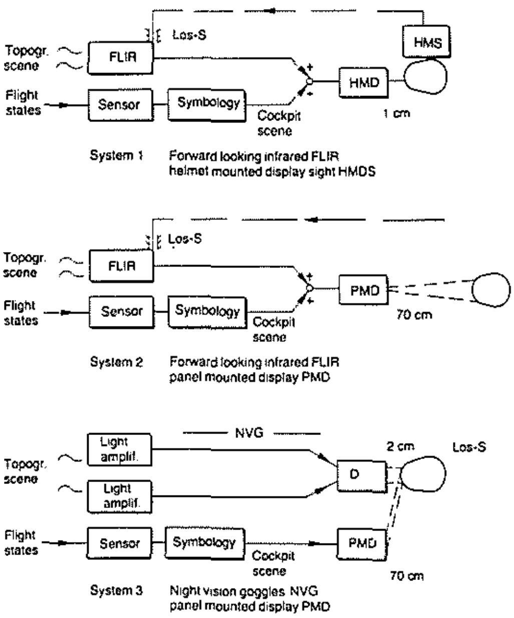

Fig. 20 Night Vision Systems Solutions

Mission I – night abilities	Mission II – night abilities	Mission III – night abilities
Take-off Departure Low level turns Cruise flight – 50 kts-V_{max} – 250-400 ft GND – Direct (WP to WP) Normal approach Short hover No position hold Touch down Taxiing	Take-off Low departure Low level turns Cruise flight – 50 kts-V_{max} – 120-250 ft GND – Terrain avoiding WP to WP Shallow approach Extended hover Position hold Touch down Taxiing	Scramble take-off Very low departure Steep Turns near the ground Cruise Flight – Hover to Vmax – 50-120 ft GND – Terrain/obstacle avoidance Approach out of NOE-flight Extended hover Position hold in the vicinity of obstacles Quick stop, running landing Taxiing

Table 4 Considered Mission Abilities

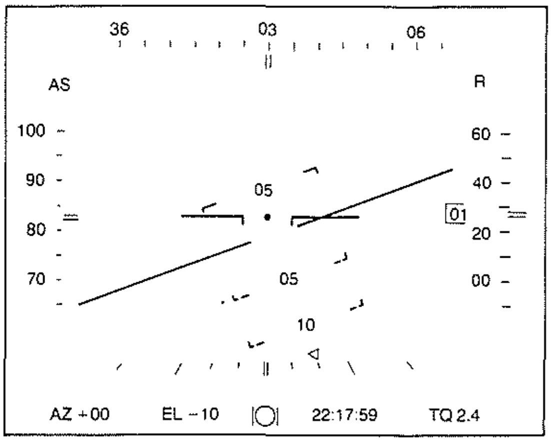

Fig. 21 NSC Cruise Symbology

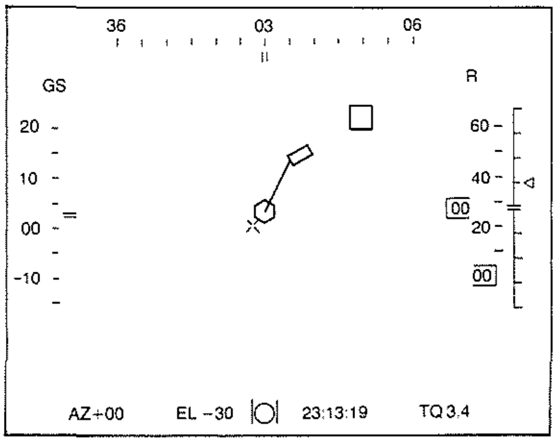

Fig. 22 NSC Hover Symbology

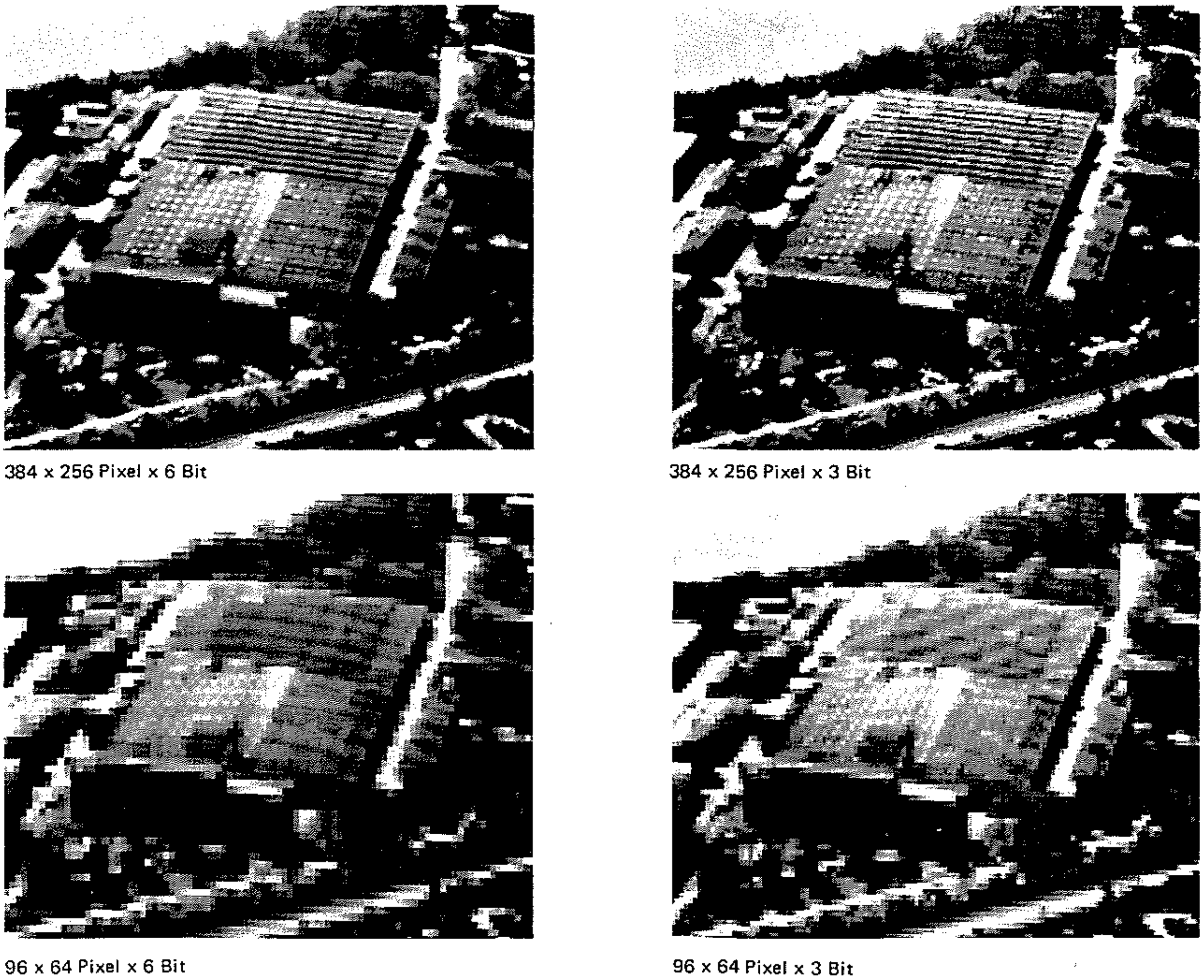

384 x 256 Pixel x 6 Bit

384 x 256 Pixel x 3 Bit

96 x 64 Pixel x 6 Bit

96 x 64 Pixel x 3 Bit

Fig. 23 Variations of Image Resolution

Image with Noise

Image Accumulation

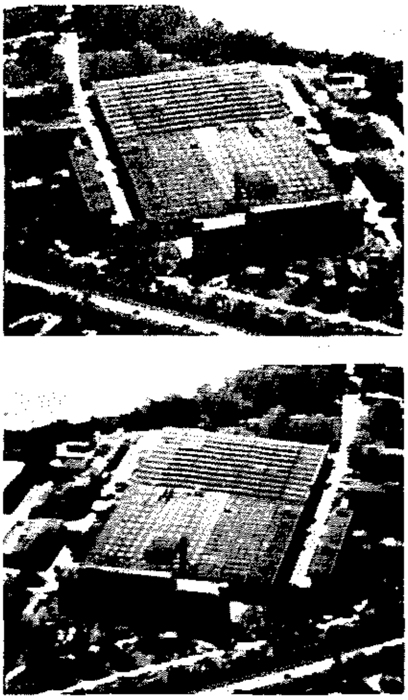

Fig. 24 Noise-Cleaning Filter

Low-Contrast Image

Histogram Equalization

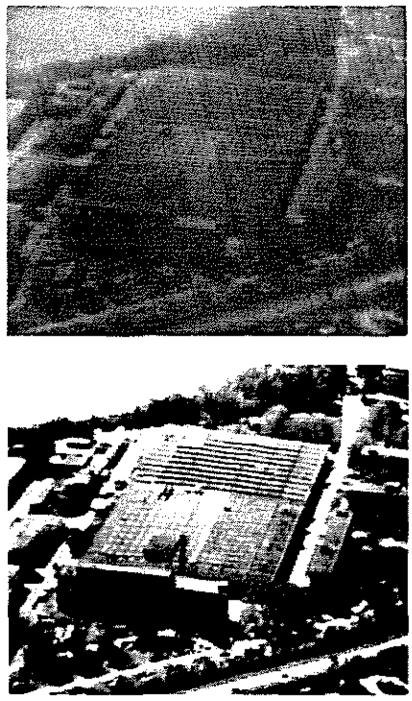

Fig. 25 Enhancement of Low-Contrast-Images

Vertical Movement Blure

Inverse Filtering

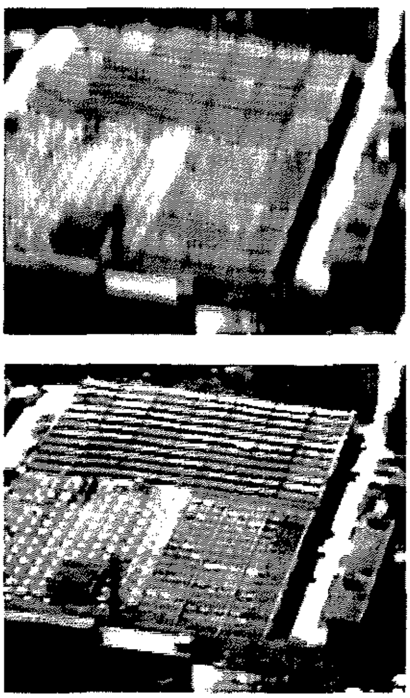

Fig. 26 Filtering of Movement Blure

Original Image

High-Pass Filter

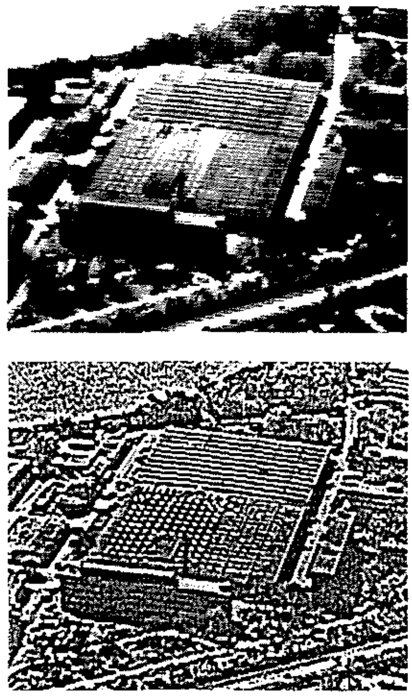

Fig. 27 High-Pass Filter

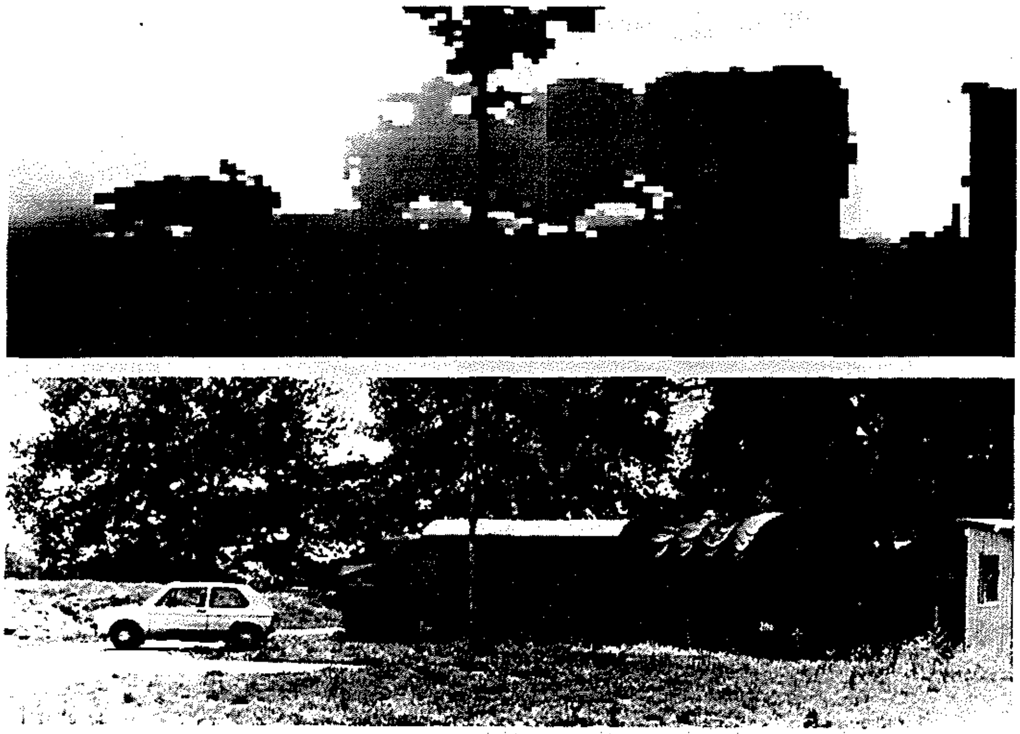

Fig. 28 Ladar Range Image